

Numerical Analysis on Run-Up of Multi-Solitary Waves on A Planar Slope

Xingjian Yan

Courant Institute of Mathematical Sciences, New York University, New York, NY, United States

Yiyang Xu

Division of Applied Mathematics, Brown University, Providence, RI, United States

Hua Liu

MOE Key Laboratory of Hydrodynamics, Shanghai Jiao Tong University, Shanghai, China

ABSTRACT

Tsunami waves transform into a series of solitary waves or undular bores over a mild slope. Nonlinear dispersion of water waves plays an important role in modeling tsunami wave propagation and deformation over varying bottom topography. This paper presents a numerical investigation on the shoaling and runup of multi-solitary waves using the fully nonlinear Boussinesq equations solved with a high-order adaptive time-stepping TVD solver (FUNWAVE-TVD). We first simulated 1-D solitary waves traveling up a slope and then validated with solitary wave runup datasets from well-controlled laboratory experiments. Numerical results show that the runup of multi-solitary waves with uniform initial amplitude over a 1:20 slope varies with each individual wave. Then, we extended the simulations of multi-solitary wave evolution and overtaking collisions over a slope for the cases of unequal initial wave amplitude. Throughout our study, we meticulously analyzed and discussed details of wave profiles and runups considering the effects of wave breaking.

KEY WORDS: Solitary wave, runup, overtaking of multi-solitary waves

INTRODUCTION

Solitary waves, by definition, are waves that maintain their shape and speed while propagating through a medium, resisting the usual tendency of waves to disperse. These waves are characterized by their stability and localized nature, often traveling over long distances without changing their fundamental structure. Solitary waves have an inherent connection with tsunamis, as tsunamis result from the runup of solitary waves, making it crucial to comprehend the dynamics of these waves and their potential collisions. Notable instances, such as the 2004 Indian Ocean tsunami and the 2011 Japan Tohoku tsunami, underscore the severe threats posed by these natural disasters, causing substantial damage and loss of life in coastal communities. Tsunamis present intrinsic dangers; therefore, analyzing the dynamics of solitary wave runup and collisions

is necessary to reveal the nearshore evolution mechanism of tsunami waves. Boussinesq equations have been applied to model solitary wave runups (Kennedy et al., 2000; Zhao, 2011), but how to deal with wave breaking, sponge layer, and shock-capturing (Choi et al., 2018) in an efficient way has been a challenge for all numerical schemes.

FUNWAVE-TVD offers a high-order adaptive time-stepping numerical scheme for solving fully nonlinear Boussinesq equations in a total variation diminishing scheme, demonstrating versatility in modeling and simulating waves, shipwakes, and tsunamis (Shi et al., 2012). It addresses wave breaking by locally employing nonlinear shallow water equations with a Froude number constraint (Liu et al., 2020). Thus, efficiently capturing dynamics on plane beaches. Most recently, it has been developed to incorporate GPU accelerations (Yuan et al., 2020).

Previous work using FUNWAVE-TVD includes N-waves and undular bores, oscillation and resonance of solitary waves upon encountering transient harbors (Gao et al., 2016a; Gao et al., 2016b), etc. However, research on solitary wave runups on slopes has been limited to single solitary wave dynamics (Ning et al., 2019) and equal-amplitude double solitary wave runups (Lo et al., 2013). Therefore, the equal-amplitude runups of three or more solitary waves on a sloped beach, along with overtaking and collisions of two or more solitary waves with different amplitudes on a sloped beach, remain to be studied through numerical simulations.

A conventional approach to runups involves experiments using wave-makers. A long-stroke wavemaker was employed to generate undulating and breaking bores, and to observe the decay of the bore based on parameters such as stroke length and wavemaker speed (Barranco and Liu, 2021; Barranco and Liu, 2023). Runup experiments on triple solitary waves with equal wave heights, along with double solitary waves with different wave heights, were conducted (Peng, 2018). Empirical formulae for free surface elevations of each solitary wave

were regressed, but the formulae lacked backing from mathematical derivations like Boussinesq equations and physical interpretations.

Therefore, in this paper and in a one-dimensional sense, we first implement FUNWAVE-TVD, transitioning from having only a single wave as the solitary wave initial condition to a superposition of finitely many solitary waves with different amplitudes at various crest locations. We then run and compare the numerical results with previously conducted experimental data (Peng, 2018; Liu et al., 2018). This examination aims to assess FUNWAVE-TVD's capability in capturing multi-solitary wave runups and overtakings.

This article is organized as follows: In Section 2, we introduce the lab experiment setup and modifications made to FUNWAVE-TVD. In Section 3, we validate the model by single solitary wave runup and qualitative results from equal-amplitude triple-solitary waves with experiment data, with a focus on the free surface elevation and wave breaking locations. In Section 4, we discuss the scenario of double solitary waves with different wave heights, with a focus on parameters determining overtaking conditions. The final section comprises the discussion and conclusions.

NUMERICAL MODEL AND VALIDATION

The data used in this paper consists of two parts: (i) experimental data obtained using wavemakers in the wave flume of the MOE Key Laboratory of Hydrodynamics at Shanghai Jiao Tong University, and (ii) numerical simulation results using the FUNWAVE-TVD model.

Numerical Model

The FUNWAVE model addresses the fully nonlinear Boussinesq equations (Shi et al., 2012):

$$\zeta_t + \nabla \cdot \mathbf{M} = 0 \quad (1)$$

$$\mathbf{M} = (h + \zeta) \left[\mathbf{u}_a + \left(\frac{z_a^2}{2} - \frac{1}{6} (h^2 - h\zeta + \zeta^2) \right) \nabla (\nabla \cdot \mathbf{u}_a) + \left(z_a + \frac{1}{h} (h - \eta) \right) \nabla (\nabla \cdot (h\mathbf{u}_a)) \right] \quad (2)$$

$$\mathbf{u}_{at} + (\mathbf{u}_a \cdot \nabla) \mathbf{u}_a + g \nabla \zeta + \mathbf{V}_1 + \mathbf{V}_2 = 0 \quad (3)$$

where $\eta = h + \zeta$ is the total water depth, ζ is the free surface elevation, g is the downwards gravitational acceleration, \mathbf{u}_a is the reference velocity and \mathbf{V}_1 and \mathbf{V}_2 are the dispersive terms defined in Kennedy et al. (2000). where $u(x, t)$ is the horizontal velocity, η is the total water depth, and $\zeta = \eta - h$ is the free surface elevation.

To facilitate a hybrid numerical scheme, the equations are rearranged, employing third-order Runge-Kutta time-stepping and the MUSCL-TVD scheme for accuracy up to fourth order within the Riemann solver. To account for wave breaking, the model seamlessly shifts to the nonlinear shallow water equations when the Froude number surpasses a specified threshold. Additionally, the model integrates a wetting-drying method for simulating a dynamic shoreline, departing from the slot method used in the previous FUNWAVE version. The code achieves parallelization through MPI with non-blocking communication.

In handling wave breaking, the FUNWAVE model locally transitions from the Boussinesq equations to the nonlinear shallow water equations when the Froude number exceeds a defined threshold. This approach enhances the accuracy of representing wave breaking phenomena. The model employs a shock-capturing breaking scheme within the numerical solver to effectively simulate wave breaking and its repercussions on coastal inundation. By dynamically switching between the Boussinesq and shallow water equations based on the Froude number criterion, the model adeptly captures the intricate behavior of breaking waves and their influence on the nearshore environment.

It thus furnishes a compilation of initial conditions for one-dimensional surface wave run-up simulations. Nevertheless, in the case of solitary waves, the coding setup is restricted to accepting only a single solitary wave characterized by a specified amplitude ($\text{Amp} = H_1$) and wave crest location ($\text{Xwavemaker} = X_1$). By making a minor adjustment through the repeated invocation of the solitary wave genesis function, we aggregate a superposition of multi-solitary wave initial conditions, generating a list of amplitude and wave crest pairs (H_i, X_i). In order to mitigate high-frequency oscillations, we modified the CFL number from its default value of 0.5 to 0.1, a modification also endorsed by Choi et al. (2018).

Initial Wave Condition of Numerical Model

The first-order conversion from wavemaker format to FUNWAVE-TVD format is as follows. A linear superposition of multi-solitary waves is used to express the profile, similar to Liu et al. (2018) and Xuan et al. (2013):

$$\frac{\zeta(x, 0)}{d} \approx \frac{H_1}{d} \text{sech}^2 [k_1(x - X_1)] + \frac{H_2}{d} \text{sech}^2 [k_2(x - X_1) + \epsilon\sigma_1] \quad (4)$$

where H_1 and H_2 are the absolute wave heights, and the wavenumbers k_1 and k_2 follow from the Grimshaw solution to the third order (Grimshaw, 1971):

$$k_i = \frac{1}{d} \cdot \sqrt{\frac{3H_i}{4d}}, i = 1, 2 \quad (5)$$

Term $\epsilon\sigma_1$, where ϵ is a constant multiple for phase σ_1 , represents the phase shift between multi-solitary wave crests in the wave making experiments. To align this phase shift with the Xwavemaker parameter in FUNWAVE-TVD, we simply introduce another location tracker $X_2 = X_1 - \frac{\epsilon\sigma_1}{k_2}$, allowing us to rewrite as follows:

$$\frac{H_2}{d} \text{sech}^2 [k_2(x - X_1) + \epsilon\sigma_1] = \frac{H_2}{d} \text{sech}^2 [k_2(x - X_2)] \quad (6)$$

As per definitions in Liu et al. (2018):

$$\sigma_1 = k_1(c_1 \cdot T_1 - S_1) \quad (7)$$

where $c_1 = \sqrt{g(H_1 + d)}$ is the traveling speed for the first solitary wave, and $T_1 = \frac{2\pi}{k_1 c_1}$ is the duration of plane motion for the first solitary wave (Lo et al., 2013). $S_1 = \frac{2H_1}{k_1 d}$ is the stroke of the first wave (Liu et al., 2018).

Hence, we have

$$X_2 = X_1 - \frac{\epsilon \sigma_1}{k_2} = X_1 - \epsilon \sqrt{\frac{H_1}{H_2}} \left(\frac{2\pi}{k_1} - \frac{2H_1}{k_1 d} \right) = X_1 - 2\epsilon \sqrt{\frac{4d^3}{3H_1}} \left(\pi - \frac{H_1}{d} \right) \quad (8)$$

Similar conversion applies to triple-solitary waves.

Validation

The experiments of multi-solitary wave runups, collision, and overtaking have been conducted at the MOE Key Laboratory of Hydrodynamics at Shanghai Jiao Tong University. Following improved Goring's wave generation methodology by Malek-Mohammadi and Testik (2010), this paper shares the same experiment setup as previous works carried out in the lab, including Liu et al. (2018) and Peng (2018). By establishing reasonable experimental models, the study measured the alongshore propagation, climbing characteristics, and breaking forms of single solitary waves, equally high multiple solitary waves, and unequally high double solitary waves on slopes. The experimental equipment and setup will be discussed in the following sections.

The facilities used in this experiment consist of a wave flume with dimensions of length, width, and height, a piston-type wave-making system (with a maximum stroke of 0.65m for the wave board), a wave gauge, a wave height acquisition system, and two high-speed cameras. On the left side of the flume is a hydraulic servo wave-maker with a piston-type wave board, and on the other end, there is an energy-dissipating slope to reduce the influence of reflected waves. The maximum working water depth of the wave flume can reach 0.8m. The solid cement slope model installed in the wave flume consists of two triangular rubber boards, with dimensions of 14m in length, 0.8m in width, and 0.7m in height. It has a gentle slope of 1/20, and its material and construction principles ensure that it does not sway or leak water during the ascent of solitary waves.

In the experiment, it is necessary to convert the programmed code into the motion speed of the paddle to determine its stroke and trajectory. By controlling the electrical signals of the control system, the operation of the wave-maker is controlled, generating water movement through the motion of the waveboard and realizing the generation of solitary waves.

A capacitive wave gauge was utilized to record the time series of the wave surface during the propagation of solitary waves. Prior to the experiment, the wave gauge underwent calibration to ensure accurate data collection. The wave gauge has a data collection frequency of 50Hz, an accuracy of 0.1mm, and a measurement range for wave height of 0.005m to 0.6m. The wave height data collected by the wave gauge are in the form of voltage signals, which can be directly converted into numerical values through the wave height acquisition system.

Two high-speed cameras were set up for the experiment to record the slope climbing and wave breaking of solitary waves. They captured the ascent and descent of solitary waves from above the slope. The cameras had a maximum frame rate of 120fps, could transfer images at 120MB/s per interface, and had a resolution of 1024x1024, enabling real-time shooting and storage. The location of solitary wave breaking was determined using rulers along the slope and high-speed camera imagery.

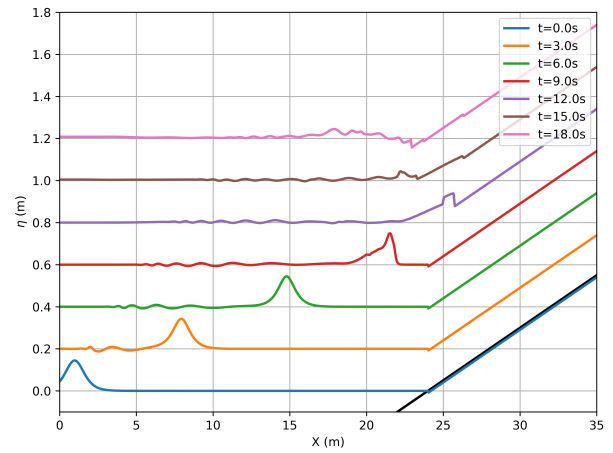
NUMERICAL RESULTS

Validation by Runup of Single- and Triple-Solitary Waves on Plane Beach

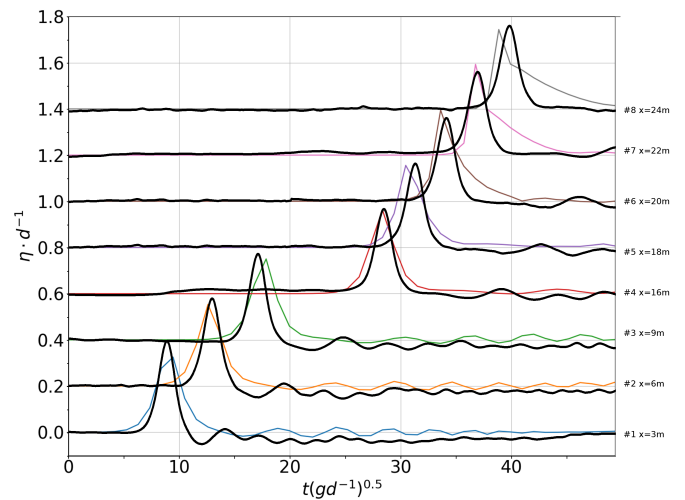
First we compare the simulation snapshots and time series of single-solitary runup with the experiment data in Peng (2018), and thus showing FUNWAVE-TVD, with wave breaking scheme being turned on, being capable of capturing single-solitary runup dynamics.

Figure 1 adopts two perspectives of this runup process: Figure 1a represents the Eulerian view at different time stamps, and Figure 1b corresponds to the wave gauge perspective of height time series at different locations.

Particularly, Figure 1b compares the simulated solitary wave with lab experiments described in Peng (2008), with black curves correspondent to the lab results, and colored curves correspondent to numerical simulations.



(a) Simulated runup snapshots of single-solitary wave



(b) Time series of free surface elevation with $d = 0.4\text{m}$ and $H/d = 0.361$

Fig. 1 Snapshots and time series of single-solitary wave

Moreover, we examined breaking location for each solitary wave in an equal-amplitude triple-solitary wave situation, with non-dimensional absolute height and phase shift being $H/d = 0.361$ and $\epsilon = 0.8$. and compared with the laboratory results shown in Peng (2018). The simulated qualitative results agree with the experimental observation that the first solitary wave breaks downstream from the breaking location of the second solitary wave. However, the model slightly differs quantitatively in the critical location where the second solitary wave starts to break. While Peng (2018) suggests the critical value to be $x = 27.4\text{m}$, the modeling results in Figure 2 showed $x \approx 24.9\text{m}$, around 9.75 seconds of propagation.

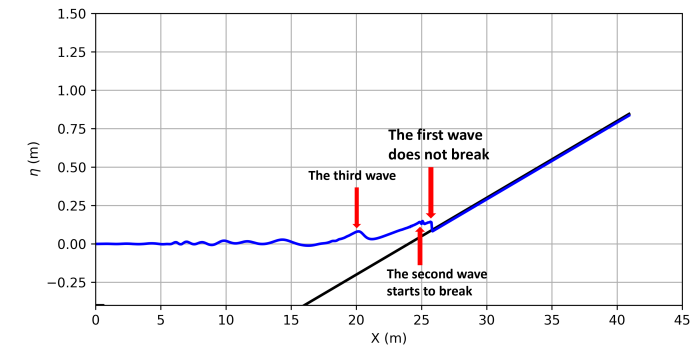


Fig. 2 Simulated breaking location for the second solitary wave

Overtaking of Double-Solitary Waves on Plane Beach

In this section, we incorporate the variation of the absolute height for individual solitary waves $H_1 \neq H_2$, which results to overtaking processes for upstream large amplitude solitary wave and downstream small amplitude solitary wave, following Liu et al. (2018):

$$c_1 = \sqrt{g(H_1 + d)} > \sqrt{g(H_2 + d)} = c_2 \tag{9}$$

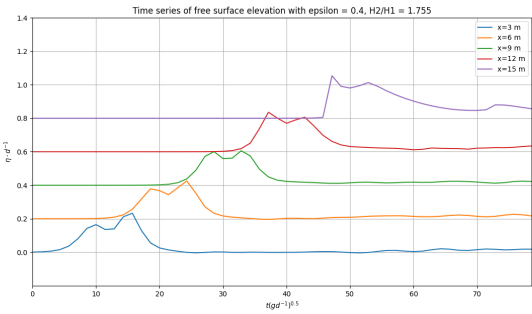
The combination of dimensional parameters for both experiments and numerical model read are provided in Table 1.

Table1: Conditions for double-solitary waves, $d = 0.3\text{m}$.

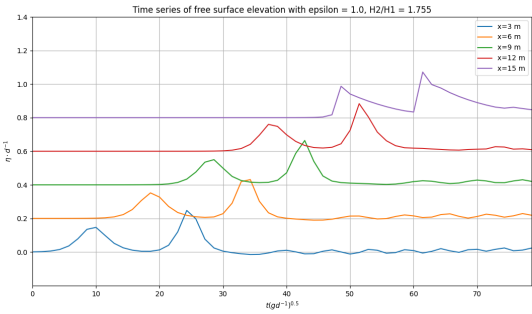
Case	H_1 (m)	H_2 (m)	ϵ	H_2/H_1
I	0.0465	0.0816	0.4	1.755
II	0.0465	0.0816	1.0	1.755
III	0.0252	0.0816	0.4	3.238
IV	0.0252	0.1113	0.4	4.417

Figure 3 shows the time series of free surface elevation of simulated double-solitary wave profiles, with parameter combination included in the table, with default $\epsilon = 0.4$.

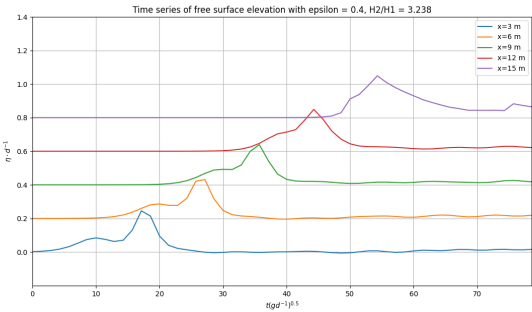
It's worth noting that, besides capturing the dynamics observed in experiments, the time series of experimental data for the free surface, measured by wave gauge 6 in Liu et al. (2018), also shows a similar flat peak occurring time for Case III as shown in Figure 4. Whereas the experiment results suggest the occurrence at $t \approx 9.97$ seconds, the numerical simulation agrees with the experimental data by displaying a relatively flat peak around $x \approx 19$ meters.



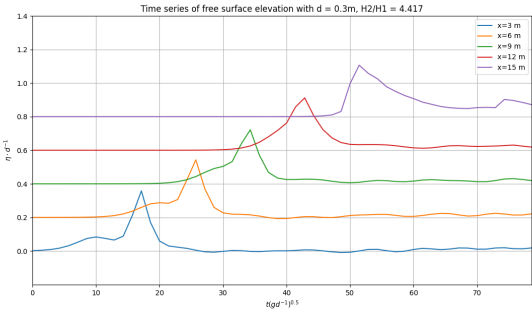
(a) Case I



(b) Case II



(c) Case III



(d) Case IV

Fig. 3 Simulated runoff snapshots of double-solitary waves.

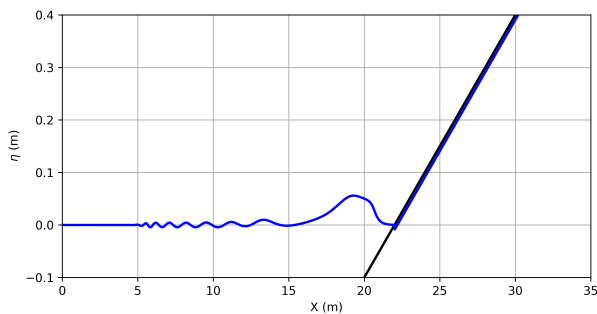


Fig. 4 Snapshot of Case III flat peak at $t = 9.75s$

A selection of snapshots of the entire overtaking process is shown in Figure 5:

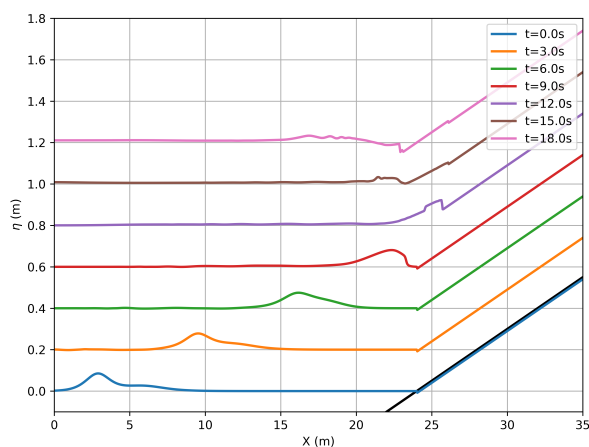


Fig. 5 Snapshots of Case III overtaking process

CONCLUDING REMARKS

Hence, we implemented, using the FUNWAVE-TVD model, numerical simulations of the propagation and runup of multi-solitary waves on a planar beach. The comparisons between lab data and the modeling results suggest that the modified FUNWAVE-TVD model is an effective tool in capturing the runup and overtaking of multi-solitary waves in the one-dimensional sense. Key qualitative results have been successfully reproduced, including the wave-breaking location for triple-solitary waves, as well as the overtaking location for specific parameters of absolute height and phase shift with reference to the sloped beach. The overall simulation results match qualitatively with observed results and only deviate quantitatively by a small amount for wave breaking location and flat peaks.

Detailed discussion on the evolution and breaking location of multi-solitary waves, and future work on the convergent runup height of a large number of solitary waves will be given in the presentation.

REFERENCES

Barranco, I, and Liu, PLF (2021). "Run-up and Inundation Generated by Non-Decaying Dam-Break Bores on a Planar Beach," *Journal of Fluid*

Mechanics, 915:A81.

Barranco, I, and Liu, PLF (2023). "Inundation, Runup and Flow Velocity of Wavemaker Generated Bores on a Planar Beach," *Journal of Fluid Mechanics*, 959:A5.

Choi, Y, Shi, F, Malej, M, and Smith, J (2018). "Performance of Various Shock-Capturing-Type Reconstruction Schemes in the Boussinesq Wave Model, FUNWAVE-TVD," *Ocean Modelling*, 131, 86-100.

Gao, J, Ji, C, Liu, Y, Gaidai, O, Ma, X, and Liu, Z (2016a). "Numerical Study on Transient Harbor Oscillations Induced by Solitary Waves," *Ocean Engineering*, 126, 467-480.

Gao, J, Ma, X, Dong, G, Wang, G, and Ma, Y (2016b). "Numerical Study of Transient Harbor Resonance Induced by Solitary Waves," *Proceedings of the Institution of Mechanical Engineers, Part M: Journal of Engineering for the Maritime Environment*, SAGE Publications, 230(1), 163-176.

Grimshaw, R (1971). "The Solitary Wave in Water of Variable Depth. Part 2," *Journal of Fluid Mechanics*, Cambridge University Press, 46(3), 611-622.

Kennedy, AB, Chen Q, Kirby, JT, Dalrymple, RA (2000). "Boussinesq Modeling of Wave Transformation, Breaking, and Runup," *Journal of Waterway, Port, Coastal, and Ocean Engineering*, 126(1), 39-47.

Liu, H, Wu, W, Peng, Y, and Fang, Y (2018). "Overtaking and Runup of Double Solitary Waves on Plane Beach," *Proc 13th Pacific-Asia Offshore Mechanics Symposium*, Jeju, ISOPE, 168-173.

Liu, W, Ning, Y, Shi, F, and Sun, Z (2020). "A 2dh Fully Dispersive and Weakly Nonlinear Boussinesq-Type Model based on a Finite-Volume and Finite-Difference TVD-Type Scheme," *Ocean Modelling*, 147, 101559.

Lo, H, Park, Y, and Liu, PLF (2013). "On the Runup and Back-Wash Processes of Single and Double Solitary Waves - an Experimental Study," *Coastal Engineering*, 80, 1-14.

Malek-Mohammadi, S, and Testik, FY (2010). "New Methodology for Laboratory Generation of Solitary Waves," *Journal of Waterway, Port, Coastal, and Ocean Engineering*, American Society of Civil Engineers, 136(5), 286-294.

Ning, Y, Liu, W, Sun, Z, Zhao, X, and Zhang, Y (2019). "Parametric Study of Solitary Wave Propagation and Runup over Fringing Reefs based on a Boussinesq Wave Model," *Journal of Marine Science and Technology*, 24(2), 512-525.

Peng, Y (2018). "An Experimental Study of Runup of Successive Solitary Waves on a Gentle Slope," Thesis, Shanghai Jiao Tong University. (in Chinese)

Shi, F, Kirby, JT, Harris, JC, Geiman, JD, and Grilli, ST (2012). "A High-Order Adaptive Time-Stepping TVD Solver for Boussinesq Modeling of Breaking Waves and Coastal Inundation," *Ocean Modelling*, 43-44, 36-51.

Xuan, R, Wu, W, and Liu, H (2013). "An Experimental Study of Runup of Two Solitary Waves on Plane Beaches," *Journal of Hydrodynamics*, 25(2), 317-320.

Yuan, Y, Shi, F, Kirby, JT, and Yu, F (2020). "FUNWAVE-GPU: Multiple-GPU Acceleration of a Boussinesq-Type Wave Model," *Journal of Advances in Modeling Earth Systems*, 12(5), e2019MS001957.

Zhao, X (2011). "Numerical Simulation of Generation, Propagation and Runup of Tsunamis," Thesis, Shanghai Jiao Tong University. (in Chinese)

Zhao, X, Liu, H, and Wang, B (2016). "Tsunami Waveforms and Runup of Undular Bores in Coastal Waters," *Journal of Engineering Mechanics*, 142(7), 06016003.

Zhong, Z, and Wang, K (2019). "A Fully Nonlinear and Weakly Dispersive Water Wave Model for Simulating the Propagation, Interaction, and Transformation of Solitary Waves," *Journal of Hydrodynamics*, 31(6), 1099-1114.